Atomic Structure of Biogenic Aragonite

B. Pokroy,[†] J. S. Fieramosca,[‡] R. B. Von Dreele,[‡] A. N. Fitch,[§] E. N. Caspi,[||] and E. Zolotoyabko*,[†]

Department of Materials Engineering, Technion-Israel Institute of Technology, Haifa 32000, Israel, Intense Pulsed Neutron Source, Argonne National Laboratory, 9700 South Cass Avenue, Argonne, Illinois 60439-4814, European Synchrotron Radiation Facility, BP 220, 38043 Grenoble Cedex, France, and Physics Department, Nuclear Research Centre, Negev, P.O. Box 9001, Beer-Sheva 84190, Israel

Received January 21, 2007. Revised Manuscript Received March 28, 2007

Atomic positions in geological aragonite and biogenic aragonite, obtained from several mollusk shells, were precisely measured by high-resolution neutron diffraction, which is more sensitive than X-ray diffraction to the positions of light atoms, C and O, in the $CaCO_3$ structure. Comparable analysis of atomic positions revealed, for the first time, the changes in some bond lengths and atomic configurations in biogenic specimens with respect to geological ones. Most pronounced are modifications in the aplanarity of the carbonate groups. These modifications correlate with the observed shifts of the ν_2 frequency in the IR absorption spectra. The changes in atomic positions as well as the changes in lattice parameters detected by high-resolution X-ray diffraction are attributed to the interaction between organic macromolecules and growing crystallites during biomineralization. The obtained results allow us deeper understanding of the specific routes used by nature for growing bio-composites with superior characteristics.

1. Introduction

Biogenic nanocomposites produced by organisms in many cases have superior properties as compared to analogous materials artificially grown in the laboratory. The improved characteristics are achieved in nature by the aid of biomacromolecules, which are deeply involved in biomineralization and are responsible for the growth mode, specific polymorph selection, orientation, and morphology of growing species.[1,2] However, despite the intensive studies, our understanding of molecular mechanisms which regulate the growth of biogenic crystals is still rather weak. Therefore, further investigations, especially with a focus on structural aspects, one of the key issues in the interaction between organic molecules and the mineral phase, are indeed required. X-ray scattering and diffraction are intensively used for this purpose to clarify phase content and microstructure of biogenic composites. Excellent examples of such studies can be found, for example, in refs 3 and 4. Concerning structural analysis, the attention was paid to modifications of lattice parameters in calcite due to magnesium impurities.[5,6] However, the effect of isomorphous substitution of Ca atoms by Mg on the contraction of lattice parameters is originated from the difference in the atomic radii of Ca and Mg and is exactly the same for biogenic and geological calcite. It is worth stressing that hitherto researchers generally do not distinguish between the atomic structure of biogenic and that of nonbiogenic crystals of the same chemical composition. Only very recently, we began systematic comparable investigation of the atomic structure of biogenic and geological crystals by using high-resolution X-ray powder diffraction measurements at synchrotron beam lines. Highly accurate structural measurements were carried out for orthorhombic aragonite and rhombohedral calcite, two polymorphs of calcium carbonate ($CaCO_3$), the most abundant mineral produced by organisms.

We found that the atomic structures of biogenic aragonite and calcite composing the mollusk shells slightly differ from the structures of chemically identical compounds of geological or synthetic origin.[6−8] Namely, in both biogenic aragonite and calcite we detected anisotropic lattice distortions reaching a maximum of about 0.2% along the *c*-axis. Nowadays similar structural distortions were also found in biogenic aragonite extracted from two different scleractinian corals.[9] By applying short-period annealing (for 30 min) at temperatures above 150 °C for aragonite and 200 °C for calcite, these lattice distortions are effectively relieved, and the lattice parameters revert closely to the values for geological aragonite or calcite.[6−8] Lattice relaxation under mild heat treatments in combination with the detected discharge of

[†] Technion-Israel Institute of Technology.
[‡] Argonne National Laboratory.
[§] European Synchrotron Radiation Facility.
[||] Nuclear Research Centre.

(1) Lowenstam, H. A.; Weiner, S. *On Biomineralization*; Oxford University Press: New York, 1989.
(2) Mann, S. *Biomineralization: Principles and Concepts in Bioinorganic Materials Chemistry*; Oxford University Press: New York, 2001.
(3) Fratzl, P.; Groschner, M.; Vogl, G.; Plenk, H.; Eschberger, J.; Fratzlzelman, N.; Koller, K.; Klaushofer, K. *J. Bone Miner. Res.* **1992**, *7*, 329−334.
(4) Wagermaier, W.; Gupta, H. S.; Gourrier, A.; Paris, O.; Roschger, P.; Burghammer, M.; Riekel, C.; Fratzl, P. *J. Appl. Cryst.* **2007**, *40*, 115−120.
(5) Magdans, U.; Gies, H. *Eur. J. Miner.* **2004**, *16*, 261−268.
(6) Pokroy, B.; Fitch, A.; Marin, F.; Kapon, M.; Adir, N.; Zolotoyabko, E. *J. Struct. Biol.* **2006**, *155*, 96−103.
(7) Pokroy, B.; Quintana, J. P.; Caspi, E. N.; Berner, A.; Zolotoyabko, E. *Nat. Mater.* **2004**, *3*, 900−902.
(8) Pokroy, B.; Fitch, A.; Lee, P.; Quintana, J. P.; Caspi, E. N.; Zolotoyabko, E. *J. Struct. Biol.* **2006**, *153*, 145−150.
(9) Stolarski, J.; Przeniosto, R.; Mazur, M.; Brunelli, M. *J. Appl. Cryst.* **2007**, *40*, 2−9.

10.1021/cm070187u CCC: $37.00
Published on Web 06/01/2007

carbon dioxide[8] allowed us to attribute the discovered lattice distortions to the intra-crystalline organic molecules that entered the mineral crystallites during biomineralization. Accurate measurements of the X-ray diffraction profiles and their modifications under annealing revealed that lattice relaxation in biogenic crystals is accompanied by a sharp reduction of the sizes of perfect crystallite blocks[10] and related increase of the averaged microstrain fluctuations.[10,11] In contrast, calcium carbonate of geological origin shows expected slow increasing of grain size under annealing[10] as is predicted by the classical grain recrystallization and growth theory (see, e.g., ref 12).

All this forced us to conclude that intra-crystalline organic molecules are located within the crystallites not randomly, like impurities, but in a regular way to be in registry with certain atomic groups. For this purpose, the molecular recognition mechanisms might be used to identify the appropriate binding sites. For example, it was suggested[13] that the molecules of glutamic acid form an ordered adsorption layer on certain facets in calcite thus lowering the surface free energy and facilitating the facet growth. In our opinion, coherent molecular attachments to favorable sites cause lattice distortions, which are revealed via precise X-ray diffraction measurements. Under heat treatments, the organic molecules degrade, and their registry with the mineral lattice is destroyed leading to the subsequent lattice relaxation and reduction in the sizes of crystal blocks which coherently scatter X-rays.

In this scenario, not only the lattice parameters but also the atomic positions within the unit cells of biogenic crystals could probably be influenced by intra-crystalline macromolecules. This is a non-trivial point, because in many practical cases the atomic positions within a deformed unit cell remain unchanged (in units of translation vectors) due to symmetry constraints. A well-known example of such a behavior provides strained semiconductor heterostructures and superlattices for band gap engineering (see, e.g., ref 14) having diamond-, sphalerite-, or wurtzite-type crystal structures. On the contrary, aragonite structure does allow some degree of freedom (within the aragonite space group) for nine atomic coordinates (see below). Probing possible changes of atomic positions in biogenic aragonite with respect to geological aragonite is the focus of the current paper. To be able to detect small changes (well below 1%) we use high-resolution neutron diffraction, which is more sensitive than X-ray diffraction to the positions of light atoms, C and O, in the presence of the heavier Ca atoms. Complementary high-resolution X-ray diffraction measurements are mostly used here to verify the neutron diffraction results for unit cell parameters. On the basis of measured atomic positions, the bond lengths and essential atomic configurations are analyzed, keeping in mind their impact on infrared characteristic frequencies.

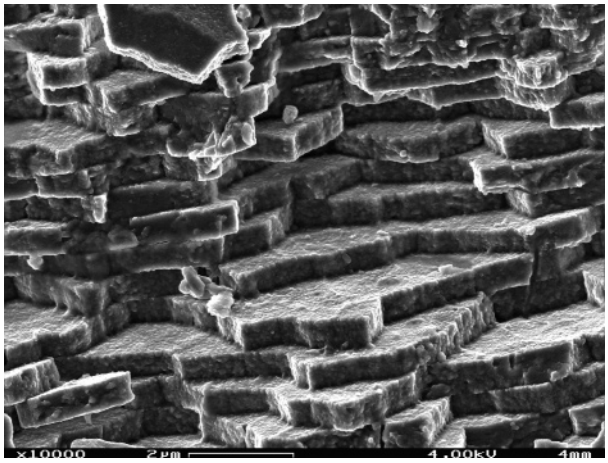

Figure 1. SEM cross section of the nacre microstructure in *Perna canaliculus*.

2. Experimental Section

Three different types of aragonitic mollusk shells, *Perna canaliculus* (bivalve), *Acanthocardia tuberculata* (bivalve), and *Strombus decorus persicus* (gastropod), were used as samples in this research. *Perna canaliculus* shell has a well-developed nacre layer, which occupies almost the entire shell volume. Scanning electron microscopy (SEM) cross section of nacre microstructure in *Perna canaliculus* is shown in Figure 1. The *Acanthocardia tuberculata* shell is composed of a rather thin (hundreds of micrometers) nacre layer and thick (up to a few millimeters) crossed-lamellar layer, while the *Strombus decorus persicus* shell is almost entirely built of crossed-lamellar layers only. The depth-dependent microstructures of the *Acanthocardia tuberculata* and *Strombus decorus persicus* shells are described in more detail in refs 15 and 16, respectively. Geological aragonite from Sefrou (Morocco), virtually free of impurities,[17] was used for comparison in structural studies. Biogenic specimens were also uncontaminated, the concentrations of most chemical impurities being well below 0.1 atom %. Only Na atoms (from seawater) were found in slightly higher concentrations reaching about 0.2 atom % at the maximum.[7] For diffraction measurements the mollusk shells, as well as geological aragonite, were cleaned by sonication in methanol and double-distilled water and then air-dried. The samples were powdered by crushing with a mortar and pestle followed by sieving through a 25 μm sieve.

High-resolution X-ray powder diffraction measurements were performed at the ID31 beam line of the European Synchrotron Radiation Facility (ESRF, Grenoble, France) equipped with a double-crystal monochromator and crystal-analyzer optical elements in the incident and diffracted beams, respectively. A description of the diffraction instrument is given in ref 18. Neutron diffraction measurements (in the time-of-flight mode) were performed at the Intense Pulsed Neutron Source (IPNS) of the Argonne National Laboratory (Argonne, IL) by using the Special Environment Powder Diffractometer (SEPD). Details of the diffraction instrument can be found in ref 19.

(10) Pokroy, B.; Fitch, A. N.; Zolotoyabko, E. *Adv. Mater.* **2006**, *18*, 2363−2368.
(11) Zolotoyabko, E.; Quintana, J. P. *J. Appl. Cryst.* **2002**, *35*, 594−599.
(12) Gottstein, G. *Physical Foundations of Materials Science*; Springer: Berlin, 2004.
(13) Teng, H. H.; Dove, P. M.; Orme, C. A.; De Yoreo, J. J. *Science* **1998**, *282*, 724−727.
(14) Jain, S. C. *Germanium-silicon strained layers and heterostructures*; Advances in Electronics and Electron Physics, Supplement; Academic Press: Boston, MA, 1994.
(15) Zolotoyabko, E.; Quintana, J. P. *Rev. Sci Instr.* **2002**, *73*, 1663−1667.
(16) Pokroy, B.; Zolotoyabko, E. *J. Mater. Chem.* **2003**, *13*, 682−688.
(17) Caspi, E. N.; Pokroy, B.; Lee, P.; Quintana, J. P.; Zolotoyabko, E. *Acta Crystallogr., Sect. B* **2005**, *61*, 129−132.
(18) Fitch, A. N. *J. Res. Natl. Inst. Stand. Technol.* **2004**, *109*, 133−142.
(19) Jorgensen, J. D.; Faber, J., Jr.; Carpenter, J. M.; Crawford, R. K.; Haumann, J. R.; Hitterman, R. L.; Kleb, R.; Ostrowski, G. E.; Rotella, F. J.; Worlton, T. G. *J. Appl. Cryst.* **1989**, *22*, 321−333.

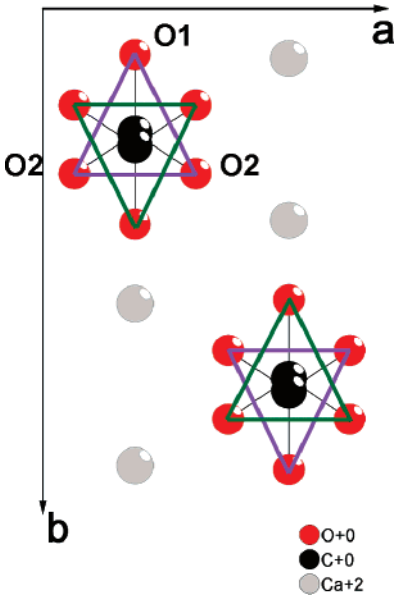

Figure 2. Projection of the aragonite unit cell on the *a*−*b*-plane showing quasi-planar carbonate groups, CO_3. Oxygen atoms (red), one O1 and two O2, form a triangle, nearly in the middle of which the C atom (black) is located.

Note that neutron diffraction measurements are time-consuming (6−18 h per diffraction pattern taken from the shell powder) as compared to synchrotron X-ray diffraction (0.5 h per diffraction pattern). For this reason, neutron diffraction was mainly applied to untreated samples (i.e., before annealing). A selected shell (*Strombus decorus persicus*) was also measured after the bleaching procedure (see next section) and after annealing for 1 h at 200 °C. The rest of the measurements were performed by means of X-ray powder diffraction.

To extract the structural parameters, the measured X-ray and neutron diffraction profiles were analyzed by means of Rietveld refinement[20] using the GSAS program[21] with the EXPGUI interface.[22]

3. Results and Discussion

Aragonite has an orthorhombic structure (space group *Pmcn*, No. 62) with the following atomic positions: Ca, C, and O1 at (4c)(1/4, *y*, *z*) and O2 at (8d)(*x*, *y*, *z*). Therefore, within the aragonite space group, *Pmcn*, six atomic coordinates could be changed for three atoms located at (4c) positions and three coordinates for O2 at (8d) positions, that is, a total of nine coordinates. Highly accurate structural parameters for geological aragonite obtained by high-resolution X-ray powder diffraction can be found in ref 17. The *x*−*y*-projection of the aragonite structure (i.e., the projection on the *a*−*b* plane) is shown in Figure 2, in which the carbonate groups composed of one C, one O1, and two O2 atoms are clearly seen. In contrast to calcite, carbonate groups in aragonite are slightly non-coplanar; that is, carbon and three oxygen atoms are not located within the same plane. This aplanarity issue is important for further analysis and will be treated in more detail below. The importance of carbonate groups in biogenic aragonite and calcite crystals is enhanced because they can be in close registry with organic molecules having the appropriate lengths of the C−O bonds.

Careful structural measurements of biogenic aragonite obtained from various mollusk shells show that it remains orthorhombic, but the lattice parameters, *a*, *b*, and *c*, differ from those for geological aragonite, demonstrating some universal behavior.[8] As an illustration, relative deviations measured in three investigated shells by means of X-ray powder diffraction are presented in histogram form in Figure 3 (left-side bars). As usual,[8] the largest and positive (i.e., tensile-like) lattice distortions, $\Delta c/c$, were found along the *c*-axis, reaching $\Delta c/c = 0.0013$ for *Acanthocardia tuberculata*, $\Delta c/c = 0.0023$ for *Perna canaliculus*, and $\Delta c/c = 0.0021$ for *Strombus decorus persicus*. Distortions of nearly half the size, but still positive, were measured along the *a*-axis, $\Delta a/a = 0.0008$, 0.0010, and 0.0011, respectively. The distortions along the *b*-axis, $\Delta b/b$, were found to be the smallest and negative (i.e., compressive-like) and equal to $\Delta b/b = -0.0004$, -0.0003, and -0.0004, respectively. Neutron diffraction results (right-side bars in Figure 3) will be discussed later on.

To eliminate a possible effect on lattice distortions from an inter-crystalline organic phase (i.e., located between crystallites), the samples were subjected to a bleaching procedure, that is, vigorous stirring in 5% sodium hypochlorite for 2 weeks that helps to remove the organic phase from between crystallites.[23] By this procedure, the interactions between inter-crystalline organic phase and a mineral are greatly diminished. In fact, these interactions apparently have almost no effect on measured lattice distortions because after the bleaching procedure the distortions are preserved essentially as before (see Figure 3, middle bars).

In contrast, annealing at elevated temperature has a dramatic effect on lattice distortions in biogenic aragonite and calcite.[6−8] Detailed experimental results for *Acanthocardia tuberculata* and *Perna canaliculus* are given in ref 8. Here we show unpublished X-ray diffraction data taken with *Strombus decorus persicus* samples annealed for 30 min at temperatures between 50 and 350 °C (see Figure 4). It is clearly seen that heat treatments above 150 °C already cause remarkable lattice relaxation. After annealing at 250 °C, the lattice parameters of *Strombus decorus persicus* revert to those of geological aragonite. The reasons for tiny distinctions, less than 5×10^{-4}, between lattice parameters of *Strombus decorus persicus* and geological aragonite, detected at higher annealing temperatures for this shell only, are not clear yet. Probably, this is the result of the considerable grain size reduction under annealing (as could be deduced from the observed diffraction peak broadening, similar to the one found in calcite)[10] and subsequent modification in the elastic-plastic interactions between 50 nm sized grains.

To compare atomic positions in biogenic and geological aragonite, we performed neutron diffraction scans with powdered samples of three different seashells as well as geological aragonite. The results of Rietveld refinements are summarized in Table 1, in which the atomic positions and

(20) Rietveld, H. M. *J. Appl. Crystallogr.* **1969**, *2*, 65−71.
(21) Larson, C.; Von Dreele, R. B. *General Structure Analysis System (GSAS)*; Report LAUR 86-748. Los Alamos National Laboratory: Los Alamos, NM, U.S.A., 1986.
(22) Toby, B. *J. Appl. Crystallogr.* **2001**, *34*, 210−221.
(23) Berman, A.; Addadi, L.; Weiner, S. *Nature* **1988**, *331*, 546−548.

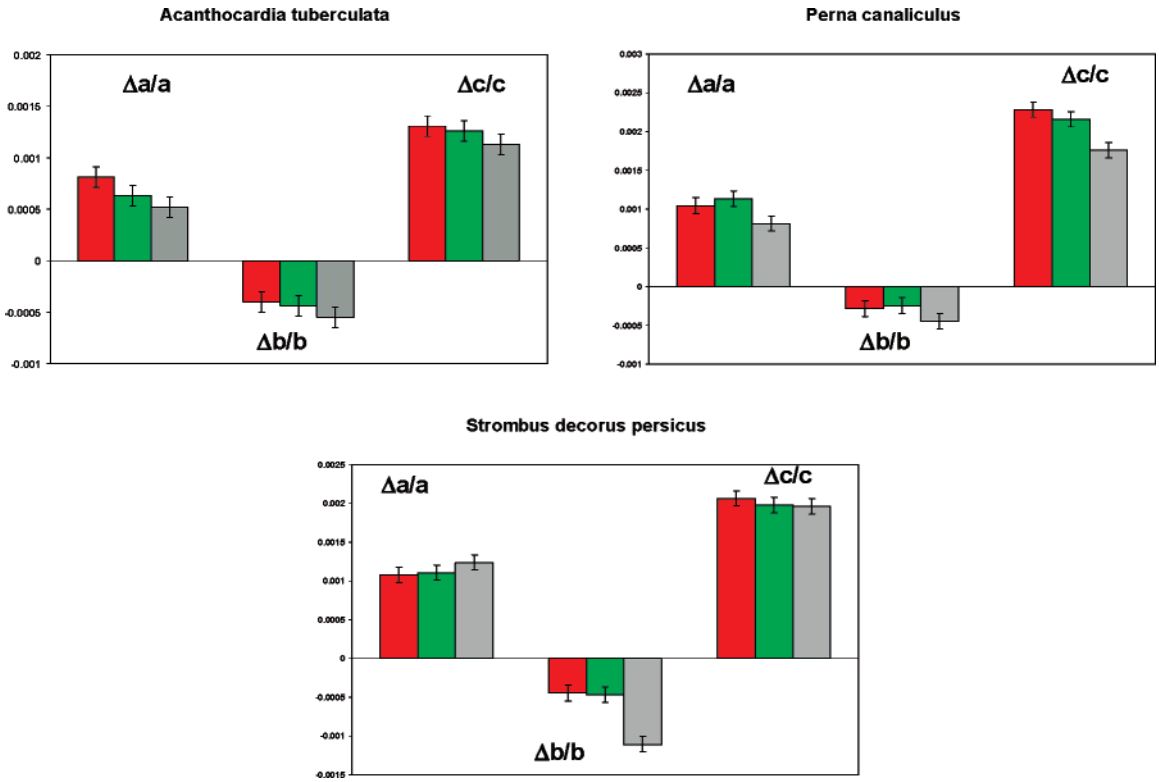

Figure 3. Anisotropic lattice distortions measured in the three investigated shells. Left-side (red) and right-side (gray) bars in each histogram represent X-ray and neutron data, respectively, taken from untreated powders. Middle bars (green) show lattice distortions after the bleaching procedure.

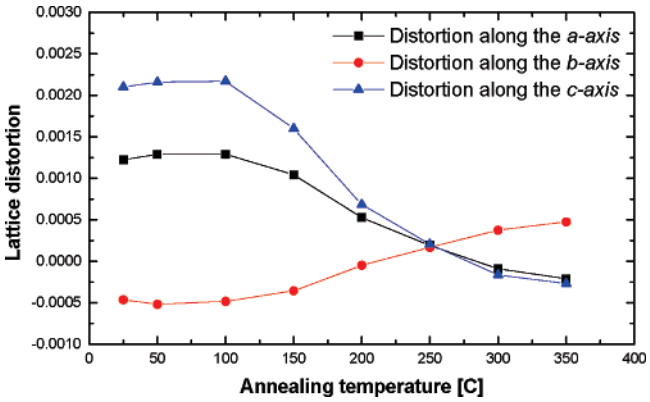

Figure 4. Annealing effect on lattice distortions in *Strombus decorus persicus*.

lattice parameters for all investigated samples are given. An example of data refinement is shown in Figure 5 (for *Strombus decorus persicus* shell).

First, we note that lattice parameters for geological aragonite extracted from X-ray[17] and neutron diffraction data coincide within 1.7×10^{-4}. This number is reasonable if the limited precision (about 10^{-4}) of absolute measurements of lattice parameters by time-of-flight neutron diffraction due to some uncertainty in the sample scattering center position is taken into account. Lattice distortions in biogenic aragonite samples probed by neutron diffraction (see Figure 3, right-side bars) are also in reasonable agreement with those measured by X-ray diffraction, especially if one takes into account that specific powders used for neutron and X-ray diffraction measurements cannot be the same, because much more material is needed for neutron diffraction measurements than for X-ray diffraction measurements. A good agreement mentioned is illustrated by the data received for *Strombus decorus persicus*, in which the largest bond length modifications were detected. For example, the highest lattice distortions at room temperature are $\Delta c/c = 0.0021$ and 0.0019, as measured by X-ray and neutron diffraction, respectively. After the bleaching procedure, this distortion remains with no change ($\Delta c/c = 0.0019$), while annealing at 200 °C causes a 10-fold reduction down to 0.0002.

Atomic positions measured by neutron diffraction in mollusk shells reveal slight deviations from those in geological aragonite, which influence the bond lengths as summarized in Table 2. The data analysis shows that a majority of bond length modifications in mollusk shells, as compared to geological aragonite, are within the measurement precision, which is about 0.3%. Substantial length variations (in excess of 1%) were detected only for the C−O1 bond (see Figure 6) and the Ca−O2 bonds (see Figure 7) in *Strombus decorus persicus*. Note that out of three different pairs of the Ca−O2 bonds in *Strombus decorus persicus* (see Table 2), the first pair is expanded by 1.3%, the second one remains practically unchanged, and the third one is contracted by −1.4%. We stress that the length modifications of certain bonds are 1 order of magnitude higher than the measured distortions of the aragonitic unit cell. Apparently, it can be understood by taking into account that bond modifications of opposite sign occur and their effect on the lattice parameters is some kind of averaging. At the same time, the effect of bleaching or annealing on bond length is not as straightforward as on lattice distortions, and some illustrative examples will be given below.

Important additional information on the structural distinctions between biogenic and geological aragonite is obtained by comparing the geometry of carbonate groups, CO_3, which

Table 1. Refined Structural Parameters of Geological and Biogenic Aragonites[a]

	geological	*Acanthocardia*	*Perna*	*Strombus*	*Strombus* bleached	*Strombus* annealed
a (Å)	4.96259(5)	4.96524(6)	4.96667(9)	4.9694(3)	4.9688(2)	4.9630(2)
b (Å)	7.96782(8)	7.9636(1)	7.9644(2)	7.9591(4)	7.9608(3)	7.9642(3)
c (Å)	5.74186(4)	5.74840(5)	5.75207(8)	5.7528(2)	5.7528(1)	5.7432(1)
			Ca			
y	0.4151(2)	0.4151(2)	0.4145(3)	0.4135(7)	0.4158(5)	0.4157(5)
z	0.7609(3)	0.7607(3)	0.7604(4)	0.7601(8)	0.7596(5)	0.7585(7)
U_{11} (Å^2)	0.0146(9)	0.0103(7)	0.012(1)	-0.001(2)	0.008(2)	0.005(2)
U_{22} (Å^2)	0.0117(9)	0.0111(8)	0.011(1)	0.020(3)	0.023(2)	0.013(2)
U_{33} (Å^2)	0.0063(7)	0.0057(7)	0.006(1)	0.002(2)	0.003(1)	0.001(2)
U_{23} (Å^2)	0.0006(6)	0.0023(6)	0.0024(9)	0.007(2)	-0.001(1)	0.000(1)
			C			
y	0.7623(1)	0.7620(1)	0.7620(2)	0.7607(4)	0.7609(3)	0.7602(3)
z	-0.0851(2)	-0.0849(2)	-0.0848(3)	-0.0851(7)	-0.0840(4)	-0.0830(5)
U_{11} (Å^2)	0.0081(5)	0.0063(5)	0.0063(7)	0.004(2)	0.007(1)	0.006(1)
U_{22} (Å^2)	0.0105(6)	0.0068(5)	0.0053(7)	0.008(2)	0.013(1)	0.006(1)
U_{33} (Å^2)	0.0077(5)	0.0066(5)	0.0093(8)	0.007(2)	0.0041(8)	0.008(1)
U_{23} (Å^2)	0.0003(6)	-0.0001(5)	-0.0006(8)	0.003(2)	-0.0001(11)	0.000(1)
			O1			
y	0.9226(2)	0.9226(1)	0.9227(2)	0.9228(4)	0.9215(3)	0.9222(4)
z	-0.0949(3)	-0.0942(3)	-0.0943(4)	-0.0905(9)	-0.09189(5)	-0.0929(7)
U_{11} (Å^2)	0.0202(9)	0.0199(8)	0.0021(1)	0.019(3)	0.023(2)	0.016(2)
U_{22} (Å^2)	0.0110(6)	0.0050(5)	0.0048(8)	-0.005(1)	0.012(1)	0.007(1)
U_{33} (Å^2)	0.0082(6)	0.0110(6)	0.010(1)	0.011(2)	0.007(1)	0.011(2)
U_{23} (Å^2)	0.0002(6)	0.0002(5)	0.0004(8)	0.002(1)	0.004(1)	0.002(1)
			O2			
x	0.4732(2)	0.4733(2)	0.4738(3)	0.4763(6)	0.4745(4)	0.4750(5)
y	0.6809(1)	0.6812(1)	0.6811(2)	0.6833(3)	0.6834(2)	0.6828(3)
z	-0.0857(2)	-0.0871(2)	-0.0866(3)	-0.0863(7)	-0.0870(4)	-0.0881(6)
U_{11} (Å^2)	0.0092(5)	0.0082(4)	0.0073(6)	0.008(2)	0.013(1)	0.011(1)
U_{22} (Å^2)	0.0147(5)	0.0123(4)	0.0133(7)	0.018(2)	0.025(1)	0.014(1)
U_{33} (Å^2)	0.0112(4)	0.0110(4)	0.0108(6)	0.007(1)	0.0069(7)	0.010(1)
U_{12} (Å^2)	0.0020(3)	0.0031(3)	0.0042(4)	0.006(1)	0.0068(7)	0.29(8)
U_{13} (Å^2)	-0.0014(4)	-0.0006(4)	-0.0007(6)	-0.002(1)	-0.0019(8)	-0.002(1)
U_{23} (Å2)	0.0015(4)	0.0018(4)	0.0012(6)	0.0009(14)	0.0032(9)	0.002(1)
R_{wp} (%)	5.37	3.53	3.30	3.17	4.63	3.36
R_{exp} (%)	4.42	2.96	2.98	2.31	3.30	2.87

[a] Atoms occupy the following positions: Ca, C, and O1 at 4c(1/4, *y*, *z*) and O2 at 8d(*x*, *y*, *z*). U_{ij} is the anisotropic thermal displacement parameter. Numbers in parentheses represent standard deviation of the last significant digits. The weighed profile (R_{wp}) and expected (R_{exp}) agreement factors are also given.

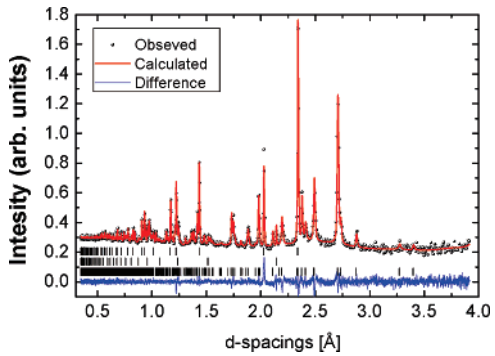

Figure 5. Neutron diffraction pattern of powdered *Strombus decorus persicus* seashell (open circles) superimposed on the best-fit calculated Rietveld refinement profile (solid line) and their difference (solid line at the bottom). Lower row of tick marks represents Bragg positions of the aragonite *Strombus decorus persicus*, while middle and upper rows are the vanadium sample holder with Al cap.

are composed of the C, O1, and two O2 atoms, visible in Figure 2. The aplanarity of carbonate groups in aragonite originates in slightly different *z*-coordinates of the C, O1, and O2 atoms (see Table 1). Taking into account that two O2 atoms possess the identical *z*- and *y*-coordinates (symmetry constraint), we plot relevant atomic positions on the *y*−*z*-projection (see Figure 8). The aplanarity of carbonate groups in biogenic and geological aragonite is clearly seen in Figure 8, showing that the C atoms in both species are located above the traces of oxygen planes (colored solid lines). This aplanarity is usually characterized by the distance, *R*, between carbon atom and oxygen plane. However, it follows from Figure 8 that this distance (black solid lines for both species) is not very sensitive for characterization of the structural distinctions between biogenic and geological aragonite. Other parameters, such as the difference in the *z*-positions for C and O1 atoms, $\Delta Z = |z(\mathrm{C}) - z(\mathrm{O1})|c$, and the inclination angle, $\gamma \ll 1$, of the oxygen plane with respect to the *z*-axis, reveal much larger variations.

For a better understanding of this fact, we derived an analytic expression for distance, *R*, via the above-mentioned parameters:

$$R = |z(\mathrm{O2}) - z(\mathrm{O1})|c \cos\gamma + \frac{|z(\mathrm{C}) - z(\mathrm{O2})|c}{\cos\gamma} - \sin\gamma\,[(y(\mathrm{O1}) - y(\mathrm{C}))b + |z(\mathrm{C}) - z(\mathrm{O2})|c \tan\gamma] \quad (1)$$

Neglecting second-order terms over γ, this finally yields

$$R \cong \Delta Z - \gamma \Delta Y \quad (2)$$

where $\Delta Y = (y(\mathrm{O1}) - y(\mathrm{C}))b$. It follows from eq 2 that the distance *R* is the difference of two terms, governed by two small parameters, ΔZ and γ. It is clear that the difference between two small quantities is less suitable to characterize

Table 2. Bond Lengths Values (in Å) in Geological Aragonite and Biogenic Aragonites from Selected Mollusk Shells [a]

bond		geological	*Acanthocardia*	*Perna*	*Strombus*	*Strombus* bleached	*Strombus* annealed
Ca−Ca	×2	3.894(2)	3.895(2)	3.891(3)	3.879(7)	3.904(5)	3.900(6)
Ca−Ca	×2	4.119(3)	4.120(3)	4.122(4)	4.127(8)	4.110(5)	4.096(6)
Ca−Ca	×2	3.940(3)	3.945(3)	3.952(4)	3.961(8)	3.952(5)	3.957(6)
Ca−C		2.905(2)	2.902(2)	2.907(3)	2.903(6)	2.891(4)	2.891(5)
Ca−C		3.249(2)	3.250(2)	3.252(3)	3.267(6)	3.245(4)	3.242(5)
Ca−C	×2	2.943(1)	2.945(1)	2.943(2)	2.944(3)	2.952(2)	2.951(3)
Ca−O1		2.418(2)	2.415(2)	2.417(3)	2.401(6)	2.401(4)	2.395(5)
Ca−O1	×2	2.659(1)	2.6615(9)	2.662(1)	2.671(3)	2.666(2)	2.658(2)
Ca−O2	×2	2.547(2)	2.547(2)	2.553(3)	2.580(6)	2.561(4)	2.559(5)
Ca−O2	×2	2.439(2)	2.449(2)	2.446(3)	2.442(5)	2.459(3)	2.462(4)
Ca−O2	×2	2.526(2)	2.521(2)	2.518(3)	2.491(6)	2.507(4)	2.502(5)
C−O1		1.278(2)	1.280(1)	1.281(2)	1.291(4)	1.279(3)	1.292(4)
C−O2	×2	1.284(1)	1.2818(9)	1.285(1)	1.282(3)	1.275(2)	1.276(2)

[a] Numbers in parentheses represent standard deviation of the last significant digits.

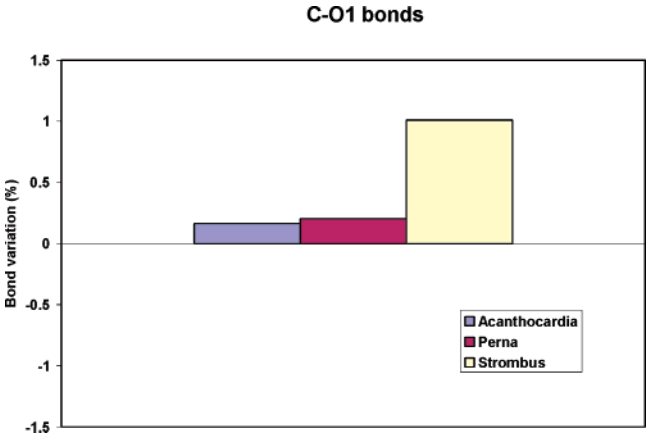

Figure 6. Length change (%) of the C−O1 bond for three investigated shells as compared to geological aragonite.

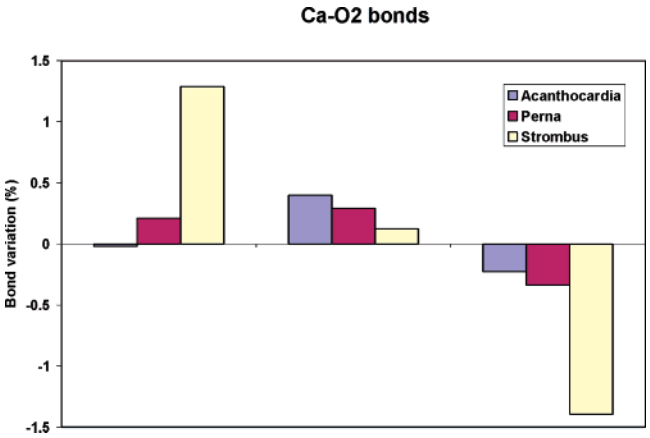

Figure 7. Length change (%) of the Ca−O2 bonds for three investigated shells as compared to geological aragonite.

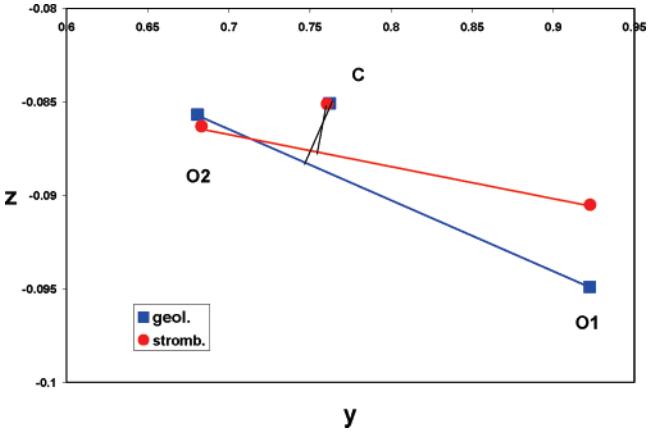

Figure 8. Geometry of carbonate groups (y−z-projection) in *Strombus decorus persicus* (in red) as compared to geological aragonite (in blue). Red and blue solid lines represent the traces of oxygen planes in these two species, respectively. Black solid lines (normals to colored ones) show R vectors.

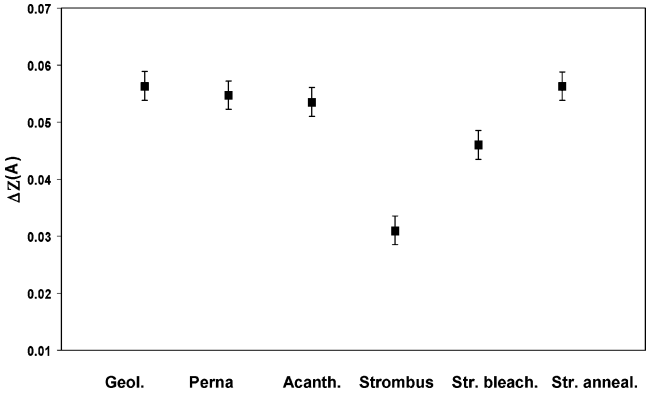

Figure 9. Distance, ΔZ, along the z-axis between C and O1 positions measured in the investigated aragonite samples by using neutron diffraction.

slight structural distinctions in biogenic crystals than the ΔZ and γ values separately.

The ΔZ and γ values calculated for all investigated biogenic and geological aragonite samples by using data from Table 1 are plotted in Figures 9 and 10, respectively. We recall here that in calcite crystals the carbonate groups are perfectly planar,[24] and ΔZ, γ, and R values equal zero. In the investigated aragonitic samples, the ΔZ value is maximal (0.056 Å) for geological aragonite and is reduced in biogenic samples. The remarkable reduction up to 0.031 Å was found for *Strombus decorus persicus*. After annealing, the ΔZ value is restored to the value of 0.056 Å, which is exactly the same as for geological aragonite. However, the bleaching procedure also is effective in increasing the ΔZ value up to 0.046 Å.

Concerning the angle, γ, maximal inclination, $\gamma = 1.57°$, was found again in geological aragonite. In the investigated biogenic crystals this angle is reduced to $\gamma = 1.31°$ in *Perna canaliculus*, $\gamma = 1.22°$ in *Acanthocardia tuberculata*, and $\gamma = 0.73°$ in *Strombus decorus persicus*. Annealing of the latter shell increases the inclination angle to $\gamma = 0.83°$, which is still considerably lower than in geological aragonite. The

(24) Maslen, E. N.; Streltsov, V. A; Streltsova, N. R. *Acta. Crystallogr., Sec. B* **1993**, *49*, 636−641.

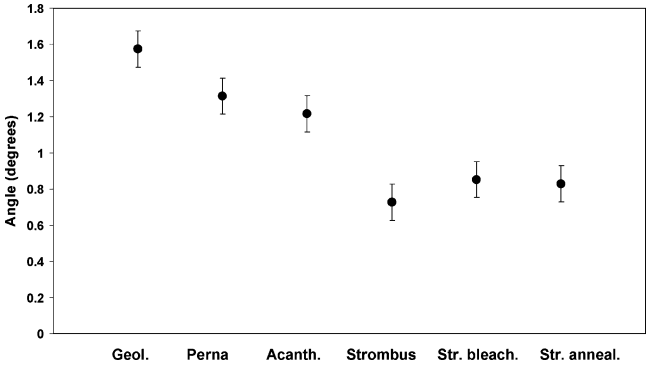

Figure 10. Angle, γ, between the O1−2 O2 oxygen plane and the *z*-axis measured in the investigated aragonite samples by using neutron diffraction.

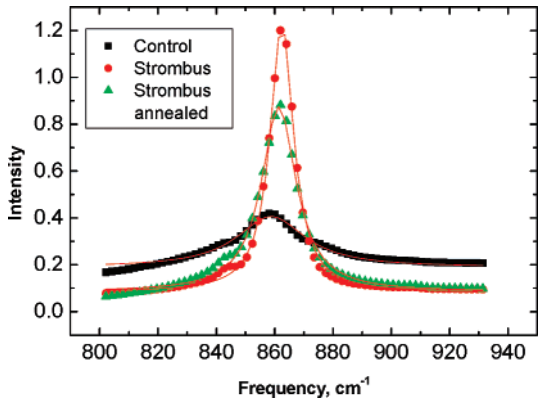

Figure 11. FTIR spectra taken in the vicinity of the ν_2 frequency from *Strombus decorus persicus* sample, before (in red) and after annealing (in green), as well as from geological aragonite (in black) for comparison.

bleaching procedure results in nearly the same value, $\gamma = 0.85°$.

Independently of fine details related to the variations of atomic positions under bleaching and annealing procedures, we expect that bond length changes in excess of 1% and clear modifications in the geometry of carbonate groups in biogenic aragonites, as compared to geological aragonite, will influence the frequencies of certain molecular vibrations. The latter could be probed by optical methods, and some preliminary results obtained by Fourier tranform infrared (FTIR) for *Strombus decorus persicus* shell are presented here. As an example, we show in Figure 11 the IR absorption spectra measured for geological aragonite and *Strombus decorus persicus* (before and after annealing) in the vicinity of the ν_2 frequency, which originates in the out-of-plane bending of carbonate groups (see, e.g., ref 25). We found that this frequency value for *Strombus decorus persicus* shell ($\nu_2 = 862.5$ cm^{-1}) is higher than that for geological aragonite ($\nu_2 = 858.8$ cm^{-1}). After annealing, the ν_2 value is reduced down to 861.4 cm^{-1}, that is, toward the value for the geological sample. An excess of the ν_2 frequency in biogenic aragonite was also documented in ref 26. In this work, the FTIR spectra taken from the crossed-lamellar layers of 16 species of aragonitic mollusk shells were statistically analyzed and compared to those taken from geological and synthetic aragonite. The mean ν_2 value of 863.4 cm^{-1} was found in biogenic aragonite, as compared to 855.5 cm^{-1} for aragonite of the non-biogenic origin. An increased ν_2 value was also reported for powdered ($\nu_2 = 863$ cm^{-1}) and unpowdered ($\nu_2 = 873$ cm^{-1}) nacre layers of red abalone.[27] According to ref 25, the ν_2 frequency increases with decreasing aplanarity of carbonate groups, reaching 879 cm^{-1} for pure calcite. Our findings fit well this tendency, if the ΔZ value or inclination angle, γ, are used to characterize the carbonate aplanarity.

4. Conclusions

Comprehensive X-ray and neutron powder diffraction measurements performed with biogenic and geological aragonite have revealed systematic deviations of the unit cell parameters in biogenic samples as compared to those in geological aragonite. By using high-resolution neutron diffraction, which is more sensitive to the positions of light C and O atoms (in the presence of heavier Ca atoms) than X-ray diffraction, we were able to measure the bond lengths with an accuracy of 0.3%. These highly accurate measurements allowed us for the first time to detect changes in certain bond lengths and atomic configurations in biogenic aragonite with respect to geological aragonite. The maximum bond length change, about 1.4%, was observed in *Strombus decorus persicus* for Ca−O2 bonds. Besides that, significant distinctions were detected in the parameters characterizing the aplanarity of carbonate groups in biogenic and geological aragonite. The changes in the bond lengths and atomic configurations should cause shifts in the IR and Raman characteristic frequencies in biogenic crystals with respect to those measured in analogous crystals of non-biogenic origin. Preliminary results obtained by FTIR in *Strombus decorus persicus* revealed a shift to higher frequency for the out-of-plane bending vibration of carbonate groups. In our opinion, this shift reflects the fact that carbonate groups in biogenic aragonite are closer to planarity than in geological aragonite, a fact which follows from neutron diffraction data. Under mild heat treatments, the majority of structural distinctions between biogenic and geological aragonite, as well as related variations in optical characteristics, are considerably reduced. The complementarities between neutron diffraction and optical (IR and Raman) measurements looks very promising for achieving a deeper understanding of local atomic structure in biogenic crystals and the role of biomacromolecules in the growth mechanisms. Note that very recently, the interrelation between local atomic order and infrared spectra in biogenic calcite was discussed in ref 28.

New findings presented in this paper strengthen our conclusion that organic molecules are more instrumental in the biomineralization process than is commonly believed. Organic molecules are not only located between crystallites, composing so named inter-crystalline organic matter in which individual crystallites are encapsulated. Apparently, spatially organized and oriented organic molecules facilitate the

(25) Healy, P. C.; White, A. H. *Spectrochim. Acta, Part A* **1973**, *29*, 1191−1195.
(26) Zhang, G. S.; Li, H. X. *Kuangwu Yanshi* **2006**, *26*, 1−4.
(27) Verma, D.; Katti, K.; Katti, D. *Spectrochim. Acta, Part A* **2006**, *64*, 1051−1057.
(28) Gueta, R.; Natan, A.; Addadi, L.; Weiner, S.; Refson, K.; Kronik, L. *Angew. Chem., Int. Ed.* **2007**, *46*, 291−294.

mineral growth from very beginning of the biomineralization process. It is reasonable to assume that these organic molecules serve as nucleation centers of calcium carbonate. Most probably, calcium carbonate initially grows as amorphous (see, e.g., refs 29−32), which facilitates reducing the strain energy caused by the mismatch-induced forces at organic−inorganic interfaces. Crystallization of amorphous calcium carbonate results in lattice distortions due to the difference in specific volumes per molecule of calcium carbonate between amorphous and crystalline phases, which acts to increase the forces imposed by organic molecules on the mineral lattice. These lattice distortions are revealed in our high-resolution diffraction measurements. Annealing at 150−200 °C leads to the degradation of organic molecules supporting the strained mineral lattice, and as a consequence, lattice relaxation to the aragonite ground state, as for pure geological crystals. The results obtained shed additional light on the complex biomineralization problem and first of all on the important and multifunctional role played by organic macromolecules in producing natural bio-composites.

(29) Levi-Kalisman, Y.; Raz, S.; Weiner, S.; Addadi, L.; Sagi, I. *Adv. Funct. Mater.* **2002**, *12*, 43−48.
(30) Becker, A.; Bismayer, U.; Epple, M.; Fabritius, H.; Hasse, B.; Shi, J.; Ziegler, A. *Dalton Trans.* **2003**, *4*, 551−555.
(31) Nassif, N.; Pinna, N.; Gehrke, N.; Antonietti, M.; Jager, C.; Colfen, H. *Proc. Natl. Acad. Sci. U.S.A.* **2005**, *102*, 12653−12655.
(32) Addadi, L.; Joester, D.; Nudelman, F.; Weiner, S. *Chem.−Eur. J.* **2006**, *12*, 980−987.

Acknowledgment. Neutron diffraction measurements were supported by the U.S. Department of Energy, Office of Science, Office of Basic Energy Sciences, under Contract No. DE-AC-02-06CH11357. X-ray diffraction measurements were partially supported by the European Synchrotron Radiation Facility. Partial support by the Israel Science Foundation and Technion V.P.R. grant is greatly appreciated.

Supporting Information Available: Crystallographic information (CIF). This material is available free of charge via the Internet at http://pubs.acs.org.

CM070187U